Contribution from the Department of Inorganic Chemistry, Indian Association for the Cultivation of Science, Calcutta 700032, India, and Department of Chemistry, Texas A&M University, College Station, Texas 77843

Ruthenium Phenolates. Chemistry of a Family of $Ru^{III}O_6$ Tris Chelates

Nilkamal Bag,[1a] Goutam Kumar Lahiri,[1a] Samaresh Bhattacharya,[1a] Larry R. Falvello,[1b] and Animesh Chakravorty*,[1a]

Received May 3, 1988

Tris chelates of ruthenium(III), RuL_3 (**2**), with *o*-formyl- and *o*-acylphenols are reported. The structure of the salicylaldehydato complex, $Ru(sal)_3$, has been determined by three-dimensional X-ray crystallography. The crystals are monoclinic in space group $P2_1/n$ with $Z = 4$ and unit cell dimensions $a = 9.718$ (2) Å, $b = 10.178$ (2) Å, $c = 18.800$ (4) Å, $\beta = 98.42$ (2)°, and $V = 1839.6$ (6) Å^3. The structure was refined to $R = 0.0332$ and $R_w = 0.0455$. The RuO_6 coordination sphere is nearly octahedral and has meridional configuration. The coordinated sal ligands are planar, but the ruthenium atom does not lie in the plane of any of the sal ligands due to a fold along the O,O line of each Ru(sal) fragment. The average Ru–O(phenolato) and Ru–O(carbonyl) distances are respectively 1.981 (2) and 2.031 (2) Å. There is a subtle form of dimerization due to two contacts of the type C–H···O between the aldehyde functions of two ligands located on two symmetry-related molecules. The low-spin ($S = {}^1/_2$) RuL_3 complexes display rhombic EPR spectra characterized by axial and rhombic distortion parameters of ~4500 and ~1500 cm^{-1}, respectively. In the axial limit the ground state of the molecule is e^4a^1. An absorption band observed near 5600 cm^{-1} is assigned to an optical transition between two Kramers doublets. Primary amines convert $Ru(sal)_3$ to Schiff base tris chelates (**4**) stereoretentively. In acetonitrile the quasi-reversible coupled $Ru^{IV}L_3^+$–$Ru^{III}L_3$ and $Ru^{III}L_3$–$Ru^{II}L_3^-$ are observed. The $Ru^{IV}L_3^+$ cation undergoes spontaneous reduction with partial ligand displacement to afford $Ru^{III}L_2(MeCN)_2^+$, which is a good synthetic precursor for complexes of the RuL_2 fragment. Reductive ligand displacement also occurs when RuL_3 reacts with 2,2′-bipyridine (bpy) in ethanol, affording $Ru^{II}L_2(bpy)$. The trivalent state can be reestablished as in $Ru^{III}(sal)_2(bpy)^+$ by oxidation with cerium(IV). The complex $Ru^{II}(sal)(bpy)_2^+$ is also reported. In the series $Ru(sal)_{3-n}(bpy)_n^z$ ($n = 0$–3), the replacement of each sal ligand by a bpy ligand shifts the ruthenium(III)–ruthenium(II) formal potential upward by ~0.6 V.

Introduction

This work stems from our interest in the chemistry of ruthenium bound to phenolic oxygen as in **1**.[2] Here A is a chelating donor

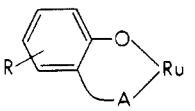

1

site ortho-linked to the aromatic ring in a direct manner or via an intervening atom (five- and six-membered chelate rings, respectively). The remarkable effect of phenolate coordination on metal oxidation states was recently revealed by the isolation of a group of 17-electron ruthenium(III) organometallics.[2a] Phenolic dioxolene complexes of ruthenium have been shown to display interesting patterns of metal and ligand oxidation levels.[3] Outside these examples only a few other types of ruthenium phenolates are known at present.[4-6]

Table I. Microanalytical Data, Bulk Magnetic Moments,[a] and EPR *g* Values[b] for RuL_3

compd	anal. data[c] % C	% H	μ_{eff}, μ_B	g_1	g_2	g_3
$Ru(sal)_3$	54.56 (54.30)	3.37 (3.23)	1.86	2.275	2.165	1.830
$Ru(Mesal)_3$	57.11 (56.91)	4.23 (4.15)	1.82	2.268	2.162	1.841
$Ru(acp)_3$	56.61 (56.91)	4.18 (4.15)	1.85	2.283	2.155	1.838
$Ru(Meacp)_3$	59.17 (59.11)	4.91 (4.93)	1.83	2.271	2.154	1.848
$Ru(prp)_3$	59.20 (59.11)	4.97 (4.93)	1.81	2.269	2.162	1.856

[a] In the solid state at 298K. [b] Measurements were made in 1:1 acetonitrile–toluene glass at 77K. [c] Calculated values are in parentheses.

Herein we explore the binding of ruthenium by salicylaldehydes and substituted derivatives thereof—phenols in which the A site is a formyl or acyl oxygen. Metal complexes of this group of ligands have a long history as rational precursors of metal salicylaldimines.[7] The chemistry of ruthenium salicylaldehydes has however not progressed so far beyond minor activities with a few assorted mixed-ligand complexes of the bivalent state.[5g,6]

The synthesis, characterization and reactivity of a new class of $Ru^{III}O_6$ tris chelates, RuL_3, afforded by the above-mentioned O,O ligands are reported in this paper. The structure of the parent salicylaldehydato complex, $Ru(sal)_3$ has been determined by X-ray crystallography. This has provided the first measures of phenolic and carbonylic Ru^{III}–O distances uncomplicated by delocalization and coligand effects. The rhombic distortion of the meridional

(1) (a) Indian Association for the Cultivation of Science. (b) Texas A&M University.

(2) (a) Lahiri, G. K.; Bhattacharya, S.; Mukherjee, M.; Mukherjee, A. K.; chakravorty, A. *Inorg. Chem.* **1987**, *26*, 3359-3365. (b) Lahiri, G. K.; Bhattacharya, S.; Ghosh, B. K.; Chakravorty, A. *Inorg. Chem.* **1987**, *26*, 4324-4331.

(3) Phenolic dioxolene complexes: (a) Boone, S. R.; Pierpont, C. G. *Inorg. Chem.* **1987**, *26*, 1769-1773. (b) Haga, M.; Dodsworth, E. S.; Lever, A. B. P.; Boone, S. R.; Pierpont, C. G. *J. Am. Chem. Soc.* **1986**, *108*, 7413-7414. (c) Haga, M.; Dodsworth, E. S.; Lever, A. B. P. *Inorg. Chem.* **1986**, *25*, 447-453. (d) Griffith, W. P.; Pumphrey, C. A.; Rainey, T. A. *J. Chem. Soc., Dalton Trans.* **1986**, 1125-1128. (e) Pell, S. D.; Salmonsen, R. B.; Abelleira, A.; Clarke, M. J. *Inorg. Chem.* **1984**, *23*, 385-387. (f) Connelly, N. G.; Manners, I.; Protheroc, J. R. C.; Whiteley, M. W. *J. Chem. Soc., Dalton Trans.* **1984**, 2713-2716. (g) Girgis, A. Y.; Sohn, Y. S.; Balch, A. L. *Inorg. Chem.* **1975**, *14*, 2327-2331.

(4) Azophenol and schiff base complexes: (a) Benson, E. P.; Legg, J. I. *Inorg. Chem.* **1981**, *20*, 2504-2507. (b) Thronback, J. R.; Wilkinson, G. *J. Chem. Soc., Dalton Trans.* **1978**, 110-115. (c) Murray, K. S.; Van den Bergen, A. M.; West, B. O. *Aust. J. Chem.* **1978**, *31*, 203-207. (d) Finney, K. S.; Everett, G. W., Jr. *Inorg. Chim. Acta* **1974**, *11*, 185-188. (e) Calderazzo, F.; Floriani, C.; Henzi, R.; L'Eplattenier, F. *J. Chem. Soc. A* **1969**, 1378-1386. Reference 2 also deals with such complexes.

(5) 8-Hydroxyquinoline complexes: (a) Kamata, Y.; Kimura, T.; Hirota, R.; Miki, E.; Mizumachi, K.; Ishimori, T. *Bull. Chem. Soc. Jpn.* **1987**, *60*, 1343-1347. (b) Gopinathan, S.; Deshpande, S. S.; Gopinathan, C. *Z. Anorg. Allg. Chem.* **1985**, *527*, 203-207. (c) Rodman, G. S.; Nagle, J. K. *Inorg. Chim. Acta* **1985**, *105*, 205-208. (d) Dormacheva, N. E.; Konstantinov, V. N.; Luchkina, S. A.; Orchinnikov, I. V. *Koord. Khim.* **1985**, *11*, 503-509. (e) Luchkina, S. A.; Sergeeva, T. P. *Russ. J. Inorg. Chem. (Engl. Transl.)* **1983**, *28*, 1466-1468. (f) Van Doorn, J. A.; Van Leeuween, P. W. N. M. *J. Organomet. Chem.* **1981**, *222*, 299-309. (g) Powell, P. *J. Organomet. Chem.* **1974**, *65*, 89-92. Reference 2b also deals with such complexes.

(6) Hydroxy aldehyde and hydroxy ketone complexes: (a) Gopinathan, S.; Joseph, K.; Gopinathan, C. *Indian. J. Chem.* **1987**, *26A*, 128-130. (b) Joseph, K.; Despande, S. S.; Pardhy, S. A.; Unny, I. R.; Pandit, S. K.; Gopinathan, S.; Gopinathan, C. *Inorg. Chim. Acta* **1984**, *82*(1), 59-61. (c) Gopinathan, S.; Pardhy, S. A.; Gopinathan, C. *Synth. React. Inorg. Met.-Org. Chem.* **1986**, *16*, 475-483.

(7) Holm, R. H.; Everett, G. W., Jr.; Chakravorty, A. *Prog. Inorg. Chem.* **1966**, *7*, 83-214.

0020-1669/88/1327-4396$01.50/0

Table II. Spectral and Electrochemical Data for RuL_3

compd	electronic spectral data[a] λ_{max}, nm (ϵ,[b] M^{-1} cm^{-1})	electrochemical data[c,d] $E°_{298}$, V (ΔE_p, mV) Ru(IV)–Ru(III)	Ru(III)–Ru(II)
$Ru(sal)_3$	1850 (40), 560[e] (3000), 410 (14500), 350[e] (9300)	1.08 (80)	−0.48 (80)
$Ru(Mesal)_3$	1800 (40), 600 (3000), 420 (14800), 355[e] (8000)	0.92 (80)	−0.59 (80)
$Ru(acp)_3$	1800 (39), 570[e] (2900), 410 (12700), 335 (10400)	0.83 (80)	−0.74 (80)
$Ru(Meacp)_3$	1750 (60), 575[e] (2400), 415 (12600), 345[e] (9900)	0.73 (80)	−0.82 (70)
$Ru(prp)_3$	1750 (34), 550[e] (2400), 410 (8800), 335 (7800)	0.81 (110)	−0.81 (120)

[a] In acetonitrile. [b] Extinction coefficient. [c] Conditions: solvent, acetonitrile; supporting electrolyte, TEAP (0.1 M); working electrode, platinum; reference electrode, SCE; solute concentration, $\sim 10^{-3}$ M. [d] Cyclic voltammetric data: $E°_{298} = 0.5(E_{pa} + E_{pc})$, where E_{pa} and E_{pc} are anodic and cathodic peak potentials, respectively; $\Delta E_p = E_{pa} - E_{pc}$; scan rate, 50 mV s^{-1}. [e] Shoulder.

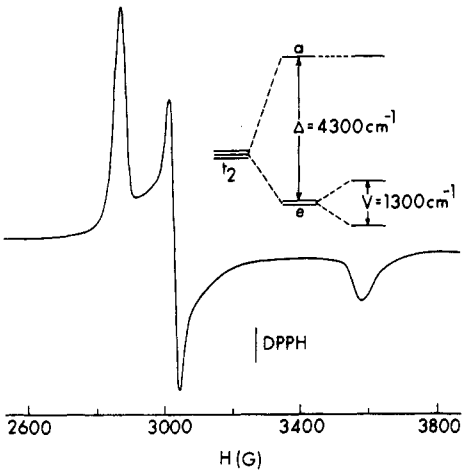

Figure 1. X-Band EPR spectrum in 1:1 acetonitrile–toluene glass (77 K) and computed t_2 splittings of $Ru(sal)_3$.

RuO_6 coordination sphere is quantitated with the help of EPR and near-IR spectroscopy. Several reactions of RuL_3 affording new complexes are explored. These include Schiff base condensation, electrochemical redox at the metal center, and redox-promoted ligand displacements.

Results and Discussion

(A) The Complexes and Their Synthesis. The five RuL_3 tris chelates synthesized in the present work and the specific abbreviations used for them are shown in **2**. Well-characterized $M(sal)_3$

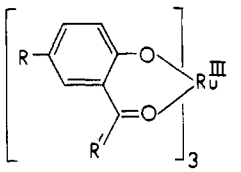

R	R′	Abbreviation
H	H	$Ru(sal)_3$
Me	H	$Ru(Me\,sal)_3$
H	Me	$Ru(acp)_3$
Me	Me	$Ru(Meacp)_3$
H	Et	$Ru(prp)_3$

2

chelates of the d-block elements are rare. The iron(III) complex, $Fe(sal)_3$ has been briefly described.[8]

The synthesis of the RuL_3 complexes was achieved by a general method: reaction of ethanol-reduced ruthenium trichloride[9] with free ligand in stoichiometric proportions in boiling ethanol. Maintenance of a slightly acidic pH (~6) by controlled addition of alkali is essential for the success of this synthesis. The dark crystalline complexes afford nonelectrolytic red solutions in organic solvents.

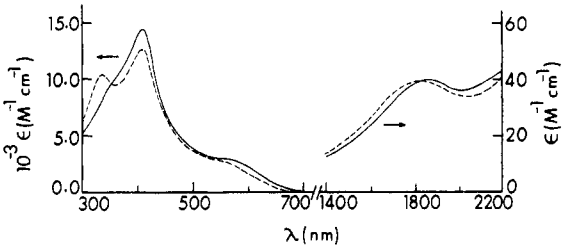

Figure 2. Electronic spectra in acetonitrile of $Ru(sal)_3$ (—) and $Ru(acp)_3$ (- - -).

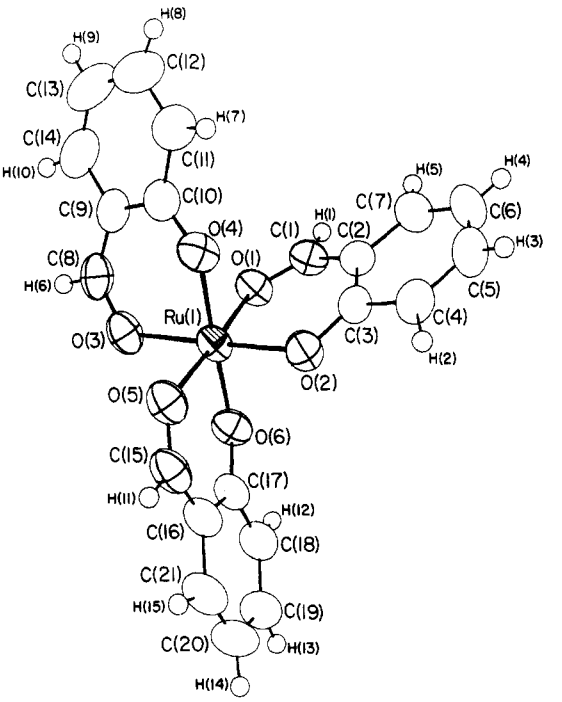

Figure 3. ORTEP drawing of the molecular structure of $Ru(sal)_3$, with the atom-labeling scheme indicated. Non-hydrogen atoms are represented by their 50% probability ellipsoids, and hydrogen atoms are shown as small circles.

(B) Characterization. Selected characterization data are set out in Tables I and II. All the complexes are low spin (t_2^5) and their magnetic moments lie in the range 1.80–1.90 μ_B. The electronic environment of the metal is rhombic as is revealed by the observation of three distinct electron spin resonance signals, (Table I, Figure 1).

The complexes have a characteristic intense absorption band near 410 nm associated with two weaker bands on two sides (~570 and ~350 nm). The origin of this absorption has not been investigated, but it may be due to LMCT excitation. A low-intensity band occurs in all complexes in the near-IR region (~1800 nm), and there are signs of another band at even lower energies (Table II, Figure 2). These bands have been assigned to ligand field

(8) Bergen, A. V. D.; Murray, K. S.; O'Connor, M. J.; Rehak, N.; West, B. O. *Aust. J. Chem.* **1968**, *21*, 1505–1515.
(9) Endo, A.; Watanabe, M.; Hayashi, S.; Shimizu, K.; Sato, G. P. *Bull. Chem. Soc. Jpn.* **1978**, *51*, 800–804.

Table III. Selected Bond Distances (Å) and Angles (deg) and Their Estimated Standard Deviations for *mer*-Ru(sal)$_3$[a]

Distances			
Ru(1)–O(1)	2.014 (2)	O(4)–C(10)	1.313 (4)
Ru(1)–O(2)	1.978 (2)	O(5)–C(15)	1.244 (5)
Ru(1)–O(3)	2.041 (2)	O(6)–C(17)	1.314 (4)
Ru(1)–O(4)	1.978 (2)	C(1)–C(2)	1.405 (4)
Ru(1)–O(5)	2.039 (2)	C(2)–C(3)	1.427 (4)
Ru(1)–O(6)	1.986 (2)	C(8)–C(9)	1.419 (5)
O(1)–C(1)	1.250 (4)	C(9)–C(10)	1.398 (5)
O(2)–C(3)	1.300 (4)	C(15)–C(16)	1.421 (5)
O(3)–C(8)	1.249 (4)	C(16)–C(17)	1.421 (5)
Angles			
O(1)–Ru(1)–O(2)	93.74 (9)	Ru(1)–O(1)–C(1)	121.0 (2)
O(1)–Ru(1)–O(3)	87.69 (9)	Ru(1)–O(2)–C(3)	122.5 (2)
O(1)–Ru(1)–O(4)	88.70 (9)	Ru(1)–O(3)–C(8)	122.6 (2)
O(1)–Ru(1)–O(5)	177.66 (9)	Ru(1)–O(4)–C(10)	122.7 (2)
O(1)–Ru(1)–O(6)	88.97 (9)	Ru(1)–O(5)–C(15)	122.8 (2)
O(2)–Ru(1)–O(3)	176.8 (1)	Ru(1)–O(6)–C(17)	124.8 (2)
O(2)–Ru(1)–O(4)	86.75 (9)	O(1)–C(1)–C(2)	129.4 (3)
O(2)–Ru(1)–O(5)	88.28 (9)	C(1)–C(2)–C(3)	124.1 (3)
O(2)–Ru(1)–O(6)	92.86 (9)	O(2)–C(3)–C(2)	125.0 (3)
O(3)–Ru(1)–O(4)	90.40 (9)	O(3)–C(8)–C(9)	128.2 (3)
O(3)–Ru(1)–O(5)	90.23 (9)	C(8)–C(9)–C(10)	122.9 (3)
O(3)–Ru(1)–O(6)	90.05 (9)	O(4)–C(10)–C(9)	125.5 (3)
O(4)–Ru(1)–O(5)	90.2 (1)	O(5)–C(15)–C(16)	129.2 (3)
O(4)–Ru(1)–O(6)	177.61 (9)	C(15)–C(16)–C(17)	123.9 (3)
O(5)–Ru(1)–O(6)	92.11 (9)	O(6)–C(17)–C(16)	124.5 (3)

[a] Numbers in parentheses are estimated standard deviations in the least significant digits.

transitions within the t_2 shell split by the rhombic nature of the ligand field; see section D.

(C) Crystal and Molecular Structure of Ru(sal)$_3$. (a) Pseudooctahedral Meridional Geometry. An ORTEP drawing of the molecule and the atom-naming scheme are displayed in Figure 3. Selected bond parameters are listed in Table III. The sal ligand acts as a bidentate O,O donor.[10-12] Since the ligand is unsymmetrical, the complex can in principle assume meridional (**3a**) and facial (**3b**) geometries. The isolated complex is exclusively meridional, and we have no evidence that the facial isomer exists.

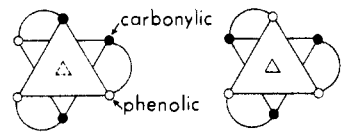

3a **3b**

The RuO_6 coordination geometry is approximately octahedral. The cis O–Ru–O angles range from 86.75 (9) to 93.74 (9)° with an average value of 90.0 (1)°. The average trans O–Ru–O angle is 177.4 (1)°. The three O_4 sets constituted by O(1), O(2), O(5), and O(3); O(1), O(6), O(5), and O(4); and O(2), O(6), O(3), and O(4) define three excellent and mutually orthogonal planes. The average dihedral angle among these is 89.75 (6)°. The ruthenium atom lies at the common intersection point of the three planes. Each *cis*-RuO_2 plane is thus a RuO_4 plane as well.

(b) Ru–O Distances. The average Ru–O(phenolato) distance is 1.981 (2) Å, which is significantly shorter than the average Ru–O(carbonyl) length, 2.031 (2) Å. The present work provides the first set of data for the latter distance in a situation where the metal is trivalent and the carbonyl function is localized. In the delocalized acelylacetone complex Ru(acac)$_3$, the average Ru–O distance is 2.00 (2) Å.[13] A few Ru^{II}–O(carbonyl) distances are known, and these lie close to 2.12 Å.[14] The Ru–O distances in Ru(sal)$_3$ can also be compared with those (averages) in the $Ru^{III}O_6$ complexes $Ru(H_2O)_3^{3+}$, 2.029 (7) Å,[15] and $Ru(C_2O_4)_3^{3-}$, 2.028 (4) Å.[16]

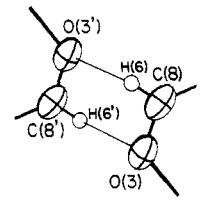

Figure 4. ORTEP drawing showing the interaction between the molecule at (x, y, z) (unprimed atom labels) and that at ($-x$, $1-y$, $-z$) (primed atom labels). Relevant distances are as follows: C(8)···O(3′), 3.044 (4) Å; C(8)–H(6), 0.91 (3) Å; H(6)···O(3′), 2.68 (3) Å; H(6)···H(6′), 3.07 (4) Å. The angle C(8)–H(6)···O(3′) is 105 (2)°.

This work has furnished, for the first time, a good measure of a normal phenolic Ru–O distance. A Ru^{III}–O(phenolato) distance of 2.112 (5) Å occurs in a ortho-metalated azophenol complex (C–Ru–O in trans configuration).[2a] The trans effect of the bound carbon atom was tentatively assigned to be the reason for the unusually long Ru–O distance, but lack of information on a normal phenolic Ru^{III}–O distances vitiated definitive assessment. The Ru(sal)$_3$ results strongly support the trans-effect hypothesis.[2a] A dioxolene complex[3a,c] has been formulated (on the basis of EPR spectra and C–O distance data) as $Ru^{II}(bpy)_2(dbsq)^+$ rather than $Ru^{III}(bpy)_2(dbcat)^+$ where db = 3,5-dibutyl, sq = semiquinone anion radical, and cat = catechol dianion. We note that the average Ru–O distance (2.048 (8) Å) in the complex indirectly supports the chosen formulation. Were the dbcat formulation correct, the oxygen atoms would be fully phenolic and the Ru–O distance would be shorter like that in Ru(sal)$_3$.

(c) sal and Ru(sal) Fragments. The coordinated sal ligands are nearly planar with only the aldehydato oxygen atom in each case lying slightly out of the plane formed by the other eight nonhydrogen atoms. That the distortions from rigid planarity are small can be seen in the relevant torsion angles—O(1)–C(1)–C(2)–C(3), 7.4 (5)°; O(3)–C(8)–C(9)–C(10), −9.2 (5)°; O(5)–C(15)–C(16)–C(17), −4.5 (6)°.

The ruthenium atom however, does not lie in the plane of any of the sal ligands—the average perpendicular deflection is 0.5 Å. This happens because each Ru(sal) fragment is folded along its O,O line. We designate the ligand with sites of chelation O(i) and O(j) as sal(i,j). The dihedral angle of the Ru,O(i), O(j) plane (which is also a RuO_4 plane, see above) with the sal(i,j) plane is 20.9 (1)° for i,j = 1,2, 25.6 (1)° for i,j = 3,4, and 14.3 (1)° for i,j = 5,6. As a result of the said distortion of the Ru(sal) fragments from planarity, the Ru(sal)$_3$ molecule as a whole seriously deviates from 3-fold symmetry. The dihedral angles sal(1,2)–sal(3,4), sal(1,2)–sal(5,6), and sal(3,4)–sal(5,6) are 127.2 (1), 97.7 (1), and 109.6 (1)°, respectively. The fold in the Ru(sal) fragment is akin to the "step"-forming distortion in bis chelates of sal.[3c,d,17]

(d) An Unusual Intermolecular Contact. In the lattice of Ru(sal)$_3$ there is a contact distance of 3.044 (4) Å between the

(10) The structures of the sal complexes of a few 3d ions are known.[11] The only structurally characterized complex of a heavier transition element appears to be that of platinum(IV).[12]

(11) (a) Garland, M. T.; LeMarouille, J. Y. *Acta Crystallogr., Sect. C.* **1985**, *C41*, 855–858. (b) Bevan, J. A.; Graddon, D. P.; McConnell, J. F. *Nature (London)* **1963**, *199*, 373. (c) McKinnon, A. J.; Waters, T. N.; Hall, D. *J. Chem. Soc.* **1964**, 3290–3294. (d) Hall, D.; McKinnon, A. J.; Waters, T. N. *J. Chem. Soc.* **1965**, 425–430. (e) Stewart, J. M.; Lingafelter, E. C.; Breazeale, J. D. *Acta Crystallogr.* **1961**, *14*, 888–891. (f) Andrew, J. E.; Blake, A. B. *J. Chem. Soc. A* **1969**, 1456–1461. (g) Pfluger, C. E.; Hon, P. K.; Harlow, R. L. *J. Cryst. Mol. Struct.* **1974**, *4*, 55–61.

(12) Truter, M. R.; Watling, R. C. *J. Chem. Soc. A* **1967**, 1955–1963.

(13) Chao, G. K.-J.; Sime, R. L.; Sime, R. J. *Acta Crystallogr., Sect. B* **1973**, *B29*, 2845–2849.

(14) (a) McGuiggan, M. F.; Pignolet, L. H. *Inorg. Chem.* **1982**, *21*, 2523–2526. (b) Abraham, F.; Nowogrocki, G.; Sueur, S.; Bremard, C. *Acta Crystallogr., Sect. B* **1980**, *36*, 779–803. (c) Bennett, M. A.; Matheson, T. W.; Robertson, G. B.; Steffen, W. L.; Turney, T. W. *J. Chem. Soc., Chem. Commun.* **1979**, 32–33.

(15) Bernhard, P.; Bürgi, H-B.; Hauser, J.; Lehmann, H.; Ludi, A. *Inorg. Chem.* **1982**, *21*, 3936–3941.

(16) Faure, P. R.; Deloume, G. D. J.-P. *Acta Crystallogr., Sect. C* **1986**, *C42*, 982–984.

(17) Holm, R. H.; O'Connor, M. J. *Prog. Inorg. Chem.* **1971**, *14*, 241–401.

Table IV. Assignments of g Values and Values of Parameters[a]

compd	g_x	g_y	g_z	k	Δ/λ	V/λ	$\Delta E_1/\lambda$	$\Delta E_2/\lambda$ calcd	$\Delta E_2/\lambda$ obsd
$Ru(sal)_3$	−2.275	−2.165	1.830	0.569	4.300	−1.304	3.718	5.271	5.405
$Ru(Mesal)_3$	−2.268	−2.162	1.841	0.569	4.439	−1.347	3.832	5.424	5.555
$Ru(acp)_3$	−2.283	−2.155	1.838	0.577	4.448	−1.593	3.738	5.538	5.555
$Ru(Meacp)_3$	−2.271	−2.154	1.848	0.572	4.577	−1.569	3.870	5.652	5.714
$Ru(prp)_3$	−2.269	−2.162	1.856	0.587	4.686	−1.477	4.012	5.718	5.714
$[Ru(sal)_2(MeCN)_2]PF_6$	−2.211	−2.211	1.811	0.533	3.954	0.000	3.732	4.593	4.902
$[Ru(sal)_2(bpy)]ClO_4$	−2.247	−2.120	1.854	0.515	4.674	−1.888	3.825	5.888	5.813

Table V. Characterization Data for Derived Complexes

compd	anal. data[a] % C	% H	% N	electronic spectral data[b] λ_{max}, nm (ϵ, M^{-1} cm^{-1})	electrochemical data[b] $E°_{298}$, V (ΔE_p, mV) Ru(III)–Ru(II)
$Ru^{III}(NBusal)_3$[c]	62.98 (62.95)	6.74 (6.68)	6.61 (6.68)	1610 (120), 550 (3200), 380 (10400), 330 (10900)	−0.97 (60)
$[Ru^{III}(sal)_2(MeCN)_2]PF_6$[d]	37.91 (37.89)	2.85 (2.81)	4.95 (4.91)	2040 (50), 725 (4400), 620 (4400), 390 (17300)	0.20 (70)
$Ru^{II}(sal)_2(py)_2$	57.41 (57.47)	3.89 (3.99)	5.51 (5.59)	600 (1400), 395 (6100)	0.31 (180)[e]
$Ru^{II}(sal)_2(PPh_3)_2$	69.17 (69.20)	4.70 (4.61)		600 (900), 405[f] (3300)	1.09[g]
$Ru^{II}(sal)_2(bpy)$	57.62 (57.70)	3.63 (3.61)	5.64 (5.61)	575 (5200), 490 (5100), 448[f] (4400), 355 (5400)	0.04 (70)
$[Ru^{II}(sal)(bpy)_2]ClO_4$[h]	51.08 (51.14)	3.38 (3.31)	8.79 (8.84)	550[f] (4900), 480 (7300), 400 (6300), 340 (8200)	0.64 (70)
$[Ru^{III}(sal)_2(bpy)]ClO_4$[i]	48.23 (48.11)	3.09 (3.01)	4.61 (4.68)	1720 (70), 655 (2200), 580[f] (2100), 390 (10500)	0.04 (70)

[a] Calculated values are in parentheses. [b] In acetonitrile. [c] μ_{eff} = 1.85 μ_B; g_1 = 2.271, g_2 = 2.124, g_3 = 1.864 in 1:1 acetonitrile–toluene (77 K); Ru(IV)–Ru(III) couple at $E°_{298}$ = 0.53 V. [d] Λ_M = 145 Ω^{-1} cm^2 M^{-1} in acetonitrile; μ_{eff} = 1.79 μ_B; g_1 = 2.211, g_2 = 2.211, g_3 = 1.811 in 1:1 acetonitrile–toluene (77 K); one irreversible response at E_{pa} = 1.57 V was observed. [e] In pyridine. [f] Shoulder. [g] E_{pa} value. [h] Λ_M = 141 Ω^{-1} cm^2 M^{-1} in acetonitrile. [i] Λ_M = 140 Ω^{-1} cm^2 M^{-1} in acetonitrile; μ_{eff} = 1.87 μ_B; g_1 = 2.247, g_2 = 2.120, g_3 = 1.854 in 1:1 acetonitrile–toluene (77 K).

aldehydic carbon atom C(8) of one ligand and the aldehydic oxygen atom O(3) of the symmetry-related molecule at $(-x, 1-y, -z)$. The angle at the hydrogen atom, C(8)–H(6)···O(3) is 105 (2)°. This interaction, which can possibly be considered as nonclassical hydrogen bonding and is displayed in Figure 4, must augment the stability of the expanded lattice and is consistent with the indications of overall tight packing in the crystal. The fact that the crystal is well packed can be seen in the differential volume value of 16.4 Å^3 per nonhydrogen atom.

(e) Structure of Other RuL_3 Species. The characterization data of Tables I and II reveal that all the RuL_3 complexes described are closely akin to $Ru(sal)_3$, and it is very reasonable to assume that they all have meridional RuO_6 coordination spheres.

(D) Electronic Structure. The X-ray results have shown that neither $Ru(sal)_3$ as a whole nor the RuO_6 coordination sphere has any symmetry. The asymmetry of ruthenium electronic environments in $Ru(sal)_3$ and other RuL_3 complexes is revealed by their rhombic EPR spectra (Figure 1, Table I). The spectra are pseudoaxial, consisting of an isolated resonance, g_3 ($g_\parallel$ in the axial limit) and two relatively closely spaced resonances, g_1 and g_2 (rhombic components of the $g_\perp$). Clearly the axial distortion (Δ) that splits the t_2 shell into a and e components is much stronger than the rhombic distortion (V), that splits e. In RuL_3 the pseudo-C_3 axis (dotted triangle in **3a**) is taken as the z axis, and we write $g_1 = |g_x|$, $g_2 = |g_y|$, and $g_3 = |g_z|$.[18] The distortion in RuL_3 can be quantitated with the help of the experimental g values and the **g** tensor theory of low-spin d^5 complexes.[19] Details of the methods used by us can be found elsewhere.[2,20]

Selected results are collected in Table IV, and additional information is deposited as supplementary material. Here λ is the spin–orbit coupling constant, k is the orbital reduction factor, and ΔE_1 and ΔE_2 are the transition energies within the Kramers doublets originating from the t_2 orbital via the application of Δ, V, and λ.[2,19,20] The axial distortion is approximately 3 times stronger than the rhombic component. The positive sign of Δ is compatible with a lying above e in the axial limit (e^4a^1 ground state). In ruthenium(III) complexes λ is ~1000 cm^{-1}.[2] Hence the computed values of ΔE_1 and ΔE_2 lie in the ranges 3700–4000 and 5300–5700 cm^{-1}, respectively. The ΔE_2 transition is indeed observed in the predicted region (Figure 2, Table IV), but the peak of the ΔE_1 transition lies outside the range of our equipment. Relatively low k values appear to be a common feature of several groups of tris chelates[2b,20b,21] including RuL_3.

(E) Reactions. The two main reactive sites in RuL_3 are the carbonyl group and the metal center. Primary amines convert the carbonyl function into the azomethine function, –CH=N–, without affecting the metal oxidation level. The trivalent state of ruthenium is optimally stabilized in RuL_3 by the O_6 environment. Metal oxidation and reduction introduces instability, leading to secondary reactions such as partial ligand displacement. Some specific details are cited below.

(a) Condensation with Primary Amines. Both aliphatic and aromatic primary amines react smoothly with $Ru(sal)_3$ in boiling ethanol, affording the tris(salicylaldiminato) complex, $Ru(NXsal)_3$ (**4**) in excellent yields. Hitherto the synthesis of **4** required ligand

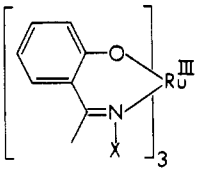

4

displacement from $Ru(acac)_3$ by preformed salicylaldimines under drastic conditions.[2b,4d] The complex $Ru(NPhsal)_3$ synthesized from $Ru(sal)_3$ is found to be identical with that obtained earlier[2b] by

(18) If the choice $g_1 = |g_y|$ and $g_2 = |g_x|$ is made the sign of rhombic parameter V (see text) is changed.

(19) (a) Bleaney, B.; O'Brien, M. C. M. *Proc. Phys. Soc., London, Sect. B* **1956**, *69*, 1216–1230. (b) Griffith, J. S. *The Theory of Transition Metal Ions*; Cambridge University Press: London, 1961; p 364.

(20) (a) Bhattacharya, S.; Chakravorty, A. *Proc.—Indian Acad. Sci., Chem. Sci.* **1985**, *95*, 159–167. (b) Bhattacharya, S.; Ghosh, P.; Chakravorty, A. *Inorg. Chem.* **1985**, *24*, 3224–3230.

(21) Desimone, R. E. *J. Am. Chem. Soc.* **1973**, *95*, 6238–6244.

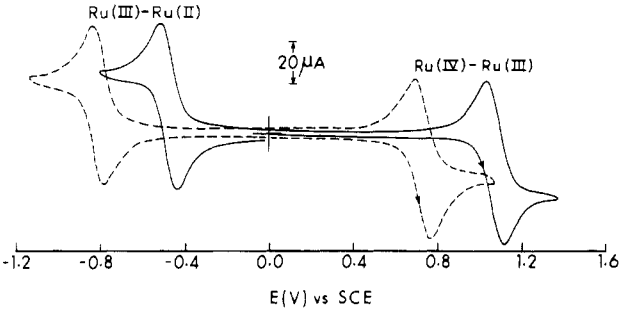

Figure 5. Cyclic voltammograms (298 K) in acetonitrile (0.1 M TEAP) at a platinum electrode of $Ru(sal)_3$ (—) and $Ru(Meacp)_3$ (---). In each case solute concentration and scan rate are $\sim 10^{-3}$ M and 50 mV s^{-1}, respectively.

the $Ru(acac)_3$ route. On the other hand X = alkyl complexes are difficult to make by the latter route in pure form. Here the $Ru(sal)_3$ method works excellently. The case of X = *n*-Bu is cited as a representative example (Table V).

In **4** the RuN_3O_3 coordination sphere has been shown to have meridional geometry.[2b] Thus the condensation of $Ru(sal)_3$ with primary amine is stereoretentive. The complex $Ru(Mesal)_3$ reacts like $Ru(sal)_3$ but the other three chelates of type **2** fail to react with primary amines, presumably because the alkyl-substituted carbonyl carbon is not sufficiently electrophilic.

(b) Electrochemical Redox. In acetonitrile solution **2** displays two one-electron cyclic voltammetric responses at the platinum electrode (Figure 5). The one-electron nature of the responses was established by current height and coulometric data. The responses are quasi-reversible with peak-to-peak separation in the range 80–120 mV. The reduction potentials shift to lower values upon alkyl substitution as expected (Table II). Between $Ru(sal)_3$ and $Ru(acp)_3$ this shift amounts to ~0.25 V. The couples at positive and negative potentials are believed to correspond respectively to metal oxidation (eq 1) and metal reduction (eq 2).

$$Ru^{IV}L_3^+ + e^- \rightleftharpoons Ru^{III}L_3 \quad (1)$$

$$Ru^{III}L_3 + e^- \rightleftharpoons Ru^{II}L_3^- \quad (2)$$

Although RuL_3^+ and RuL_3^- are observable on the cyclic voltammetric time scale, both species are quite unstable and could not be characterized. The decomposition products of RuL_3^- have evaded identification. The case of RuL_3^+ is however tractable as shown below.

(c) Ligand Displacement from Oxidized Complex. Coulometrically oxidized solution of $Ru(sal)_3$ shows no trace of the original tris chelate voltammogram, proving that RuL_3^+ has decomposed. A new nearly reversible one-electron-reductive response is observed at ~0.2 V (Table V). This is due to the bluish green species $[Ru^{III}(sal)_2(MeCN)_2]^+$, which has been quantitatively isolated as the PF_6^- salt from the oxidized solution. It displays axial EPR spectrum that can be analyzed in the usual manner (Table IV). It is an excellent starting material for the synthesis of species of type $Ru(sal)_2D_2$ (D = py, PPh_3, etc.). The stereochemistry of the cation (at present believed to have $Ru(MeCN)_2$ in a trans geometry), the pathway of its formation from RuL_3^+, and the chemistry of the various derived species are under scrutiny. The behavior of other RuL_3 complexes is parallel to that of $Ru(sal)_3$.

(d) Ligand Displacement Associated with Metal Reduction. In boiling ethanol 2,2′-bipyridine (bpy) displaces one sal ligand from $Ru(sal)_3$ (other RuL_3 complexes behave similarly) with concomitant metal reduction, affording the violet diamagnetic complex $Ru^{II}(sal)_2(bpy)$ in high yield. Presumably ethanol is the reductant in this reaction, which fails to proceed in solvents like benzene and acetonitrile. Only one sal ligand is replaced even when bpy is present in excess. However, the red cationic complex $Ru^{II}(sal)(bpy)_2^+$ (isolated as the perchlorate salt) can be synthesized by reacting $Ru(bpy)_2CO_3$ with salicylaldehyde in ethanol.

The ruthenium(III)–ruthenium(II) reduction potential systematically shifts (Tables II and V) to higher values as sal is progressively replaced by bpy; in $Ru(bpy)_3^{2+}$ the potential is 1.30 V.[22] The shift per replacement is 0.60 V. The ruthenium(III) congener (Table V) of $Ru(sal)_2(bpy)$ can be isolated as the perchlorate salt via oxidation by cerium(IV). Its rhombic EPR spectrum has been analyzed in terms of Δ and V parameters, and the ΔE_2 transition is observable (Table IV). There is no dramatic change in the distortion parameters upon substitution of a sal in $Ru(sal)_3$ by bpy.

(F) Concluding Remarks. Tris(salicylaldehydato)ruthenium(III) and some of its substituted derivatives have been synthesized. Structural characterization of $Ru(sal)_3$ has revealed exclusive meridional geometry. The phenolic Ru^{III}–O distance is found to be significantly shorter than the carbonyl Ru^{III}–O distance. It is believed that these distances can be used as standards in examining other ruthenium systems having phenolic and/or carbonyl coordination. The electronic environment in RuL_3 is strongly distorted from the O_h geometry. In the idealized trigonal limit the ground-state configuration is e^4a^1. The complexes are reactive and act as good starting materials for synthesis of other types of species via Schiff base condensation and redox-regulated ligand displacement. Ongoing studies include structural characterization of some of the species such as $Ru(sal)_2(MeCN)_2^+$, and $Ru(sal)_2(bpy)^{0,+}$, with reference to geometric structure and, in particular, the pattern of Ru–O distances.

Experimental Section

Materials. Ruthenium trichloride received from Arora-Matthey, Calcutta, India, was converted to $RuCl_3 \cdot 3H_2O$ by repeated evaporation to dryness with concentrated hydrochloric acid.[23] The $Ru(bpy)_2CO_3$ complex and the MesalH ligand were prepared according to the reported procedures.[24,25] The other ligands were obtained from Aldrich Chemical Co., Inc. BDH silica gel (60–120 mesh) was used for chromatography. Purification of solvents and preparation of tetraethylammonium perchlorate for electrochemical work was done as before.[2b] Dinitrogen gas was purified by successively bubbling it through alkaline dithionite and concentrated sulfuric acid. All other chemicals and solvents were reagent grade commercial materials.

Physical Measurements. UV–vis–near-IR spectra were recorded by using a Hitachi 330 spectrophotometer. Infrared (4000–300 cm^{-1}) spectra were taken on a Perkin-Elmer 783 spectrophotometer. The magnetic susceptibility was measured on a PAR 155 vibrating-sample magnetometer fitted with a Walker Scientific L75FBAL magnet. Electrochemical measurements were done by using the PAR Model 370-4 electrochemistry system incorporating the following instruments: Model 174A polarographic analyzer, Model 175 universal programer, Model RE0074 XY recorder, Model 173 potentiostat, Model 179 digital coulometer, and Model 377 cell system. All experiments were performed under dinitrogen atmospheres. A planar Beckman Model 39273 platinum-inlay working electrode, a platinum-wire auxiliary electrode, and an aqueous saturated calomel reference electrode (SCE) were used. A platinum-gauze working electrode was used in coulometric experiments. All cyclic voltammetric data were collected at 298 K and are uncorrected for junction potentials. EPR measurements were made with a Varian Model 109CE-line X-band spectrometer fitted with a quartz dewar for measurements at 77 K (liquid dinitrogen). All spectra were calibrated with the help of DPPH (g = 2.0037). Microanalyses (C,H,N) were done by using a Perkin-Elmer 240C elemental analyzer.

Treatment of EPR Data. The procedure can be found in our recent publications.[2,20]

Preparation of Complexes. Tris(salicylaldehydato)ruthenium(III), Ru(sal)$_3$. $RuCl_3 \cdot 3H_2O$ (100 mg, 0.38 mmol) was dissolved in ethanol (30 mL), and the solution was evaporated nearly to dryness on a steam bath. The blue residue thus produced was dissolved in 1:1 ethanol–water (30 mL). The pH of this solution was adjusted to 6 by use of a dilute NaOH solution. Salicylaldehyde (163 mg, 1.33 mmol) was added to it, and the mixture was refluxed for 4 h. The red solution thus produced was evaporated to dryness in air. The solid mass obtained was dissolved in a small volume of dichloromethane and was subjected to chromatography on a silica gel column (20 × 1 cm). On elution with benzene, a yellow band separated out and was rejected. A red band was then eluted with acetonitrile–benzene (1:9). The collected eluant was evaporated to afford

(22) Tokel-Takvoryan, N. E.; Hemingway, R. E.; Bard, A. J. *J. Am. Chem. Soc.* **1973**, *95*, 6582–6589.
(23) Chakravarty, A. R.; Chakravorty, A. *Inorg. Chem.* **1981**, *20*, 275–278.
(24) Johnson, E. C.; Sullivan, B. P.; Salmon, D. J.; Adeyemi, S. A.; Meyer, T. J. *Inorg. Chem.* **1978**, *17*, 2211–2215.
(25) Duff, J. C. *J. Chem. Soc.* **1941**, 547–550.

a dark red crystalline solid. Yield: 75%.

The complexes $Ru(Mesal)_3$, $Ru(acp)_3$, $Ru(Meacp)_3$, and $Ru(prp)_3$ were prepared similarly. Yields varied in the range 70–75%.

Tris(*N*-butylsalicylaldiminato)ruthenium(III), Ru(NBusal)$_3$. $Ru(sal)_3$ (100 mg, 0.22 mmol) in *n*-butylamine (55 mg, 0.75 mmol) were taken up in ethanol (30 mL) and the mixture was refluxed for 4 h. The reddish-green solution thus produced was evaporated to dryness under reduced pressure. The solid was dissolved in a small volume of benzene and subjected to chromatography on a silica gel column (20 × 1 cm). A yellow band was eluted with benzene and was rejected. A reddish green band was then eluted with benzene–acetonitrile (3:1). The eluant was evaporated under reduced pressure to yield a crystalline solid. Yield: 65%.

The complex $Ru(NPhsal)_3$ was prepared (yield 60%) by an entirely analogous method using aniline instead of *n*-butylamine. This complex was found to be identical with that reported earlier.[2b]

Bis(acetonitrile)bis(salicylaldehydato)ruthenium(III) Hexafluorophosphate, $[Ru(sal)_2(MeCN)_2]PF_6$. $Ru(sal)_3$ (100 mg, 0.22 mmol) was oxidized coulometrically in acetonitrile (0.1 M in NH_4PF_6) at 1.20 V. After the oxidation was over (coulomb count corresponding to one electron), the bluish green solution was evaporated to dryness under reduced pressure. The solid mass thus obtained was washed thoroughly with cold water to remove NH_4PF_6 and dried in vacuo over P_4O_{10}. The yield was quantitative.

Bis(pyridine)bis(salicylaldehydato)ruthenium(II), Ru(sal)$_2$(py)$_2$. Pyridine (2 mL) was added to $[Ru(sal)_2(MeCN)_2]PF_6$ (100 mg, 0.18 mmol), and the mixture was stirred magnetically for 30 min. The red-brown solution thus produced was evaporated to dryness under reduced pressure. The solid mass was dissolved in benzene and chromatographed through a silica gel column (20 × 1 cm). A red-brown band eluted with benzene and was collected and evaporated to afford a dark crystalline solid. Yield: 60%.

Bis(triphenylphosphine)bis(salicylaldehydato)ruthenium(II), Ru(sal)$_2$(PPh$_3$)$_2$. $[Ru(sal)_2(MeCN)_2]PF_6$ (100 mg, 0.1 mmol) and triphenylphosphine (115 mg, 0.44 mmol) were taken up in ethanol (30 mL), and the mixture was refluxed for 4 h. The light brown solution thus produced afforded a crystalline solid on evaporation, which was collected by filtration, washed with water followed by ether, and dried under vacuo over P_4O_{10}. Yield: 65%.

(2,2′-Bipyridine)bis(salicylaldehydato)ruthenium(II), Ru(sal)$_2$(bpy). To $Ru(sal)_3$ (100 mg, 0.22 mmol) in ethanol (30 mL) was added 2,2′-bipyridine (50 mg, 0.32 mmol) and the mixture was refluxed for 3 h. The violet solution was evaporated to dryness under reduced pressure. The solid mass obtained was dissolved in dichloromethane and chromatographed on a silica gel column (20 × 1 cm). A yellow band that eluted with benzene was rejected. The next violet band eluted with benzene–acetonitrile (3:1) and was collected, and the solvent was evaporated to afford crystalline solid. Yield: 80%.

Bis(2,2′-bipyridine)(salicylaldehydato)ruthenium(II) Perchlorate, [Ru(sal)(bpy)$_2$]ClO$_4$. $Ru(bpy)_2CO_3$ (100 mg, 0.21 mmol) was taken up in ethanol (30 mL) to which was added salicylaldehyde (40 mg, 0.33 mmol). The mixture was refluxed for 1 h. The red solution was cooled to room temperature (298 K), and saturated aqueous $NaClO_4$ solution (10 mL) was added to it. A crystalline solid appeared, which was collected by filtration, washed thoroughly with water, and dried in vacuo over P_4O_{10}. Yield: 90%.

(2,2′-Bipyridine)bis(salicylaldehydato)ruthenium(III) Perchlorate, [Ru(sal)$_2$(bpy)]ClO$_4$. $Ru(sal)_2(bpy)$ (100 mg, 0.20 mmol) was dissolved in acetonitrile (20 mL). To this was added ceric ammonium sulfate (150 mg, 0.24 mmol) in 0.1 M $HClO_4$ (20 mL). The mixture was stirred magnetically for 30 min. To the resulting bluish green solution was added a saturated aqueous solution of $NaClO_4$ (10 mL). The green solid thus obtained was collected by filtration, washed with water, and dried in vacuo over P_4O_{10}. Yield: 90%.

Preparation of Crystals of Ru(sal)$_3$ for X-ray Analysis. Hexane (30 mL) was layered over a solution of 50 mg of $Ru(sal)_3$ in 25 mL of pure dichloromethane. Dark red crystals deposited within a few days upon very slow evaporation.

X-ray Structure Determination. X-ray diffraction data were taken from a black crystal that was mounted at the end of a glass fiber and covered with a thin layer of epoxy. Data collection procedures were routine and have been described previously.[26] Significant crystal data and data collection parameters are summarized in Table VI. Data reduction was carried out by standard algorithms.[27] An empirical absorption correction was applied,[28] based on azimuthal scans of six reflections with diffractometer angle χ near 90°. During the course of intensity data collection, two monitor reflections were measured after everey 98 data scans. These showed no significant change in intensity during an accumulated X-ray exposure time of 59.6 h.

The lattice dimensions and Laue group were checked by normal-beam axial photography, which was done for the unit cell axes and body and face diagonals. Systematic absences from the data set uniquely identified the space group as $P2_1/n$.

The position of the unique ruthenium atom was deduced from a Patterson map, and the remainder of the structure was developed and refined in an alternating sequence of least-squares calculations and difference Fourier maps. All hydrogen atoms were located in a difference map and were refined freely with individual isotropic displacement parameters. The final refinement fitted a model comprising a scale factor, 28 anisotropic, non-hydrogen atoms, and 15 isotropic hydrogen atoms—313 variable parameters in all—to 2760 data, for a data-to-parameter ratio of 8.8. Residuals from the final, convergent refinement are summarized in Table VI. No significant correlation was observed in the final refinement; and listings of R values as functions of data collection order, $(\sin\theta)/\lambda$, and crystallographic indices showed no systematic effects. Following the final refinement, the highest difference Fourier peak (1.3 e/Å^3) and the second highest peak (0.5 e/Å^3) both were ghosts of the ruthenium atom. These can be attributed to series-termination or residual absorption effects. Atomic coordinates and isotropic-equivalent

Table VI. Crystallographic Data for *mer*-$Ru(sal)_3$

chemial formula: $RuO_6C_{21}H_{15}$	$Z = 4$
fw: 464.42	$T = 26 \pm 3$ °C
space group: $P2_1/n$	$\lambda = 0.71073$ Å
$a = 9.718$ (2) Å	$\rho_{calcd} = 1.68$ g cm^{-3}
$b = 10.178$ (2) Å	$\mu = 8.74$ cm^{-1}
$c = 18.800$ (4) Å	transmissn coeff = 1.00–0.94
$\beta = 98.42$ (2)°	$R^a = 0.0332$
$V = 1839.6$ (6) Å^3	$R_w^b = 0.0486$

$^a R = \sum||F_o| - |F_c||/\sum|F_o|$. $^b R_w = [\sum w(|F_o| - |F_c|)^2/\sum w|F_o|^2]^{1/2}$; $w = 1/\sigma^2(|F_o|)$.

Table VII. Atomic Positional Parameters and Equivalent Isotropic Displacement Parameters and Their Estimated Standard Deviations for *mer*-$Ru(sal)_3$

atom	x	y	z	B,[a] Å^2
Ru(1)	0.20344 (3)	0.26955 (3)	0.07723 (1)	3.736 (5)
O(1)	0.2142 (2)	0.4450 (2)	0.1273 (1)	4.11 (4)
O(2)	0.3557 (2)	0.1923 (2)	0.1458 (1)	4.35 (5)
O(3)	0.0389 (2)	0.3416 (2)	0.0084 (1)	4.75 (5)
O(4)	0.0760 (3)	0.2089 (2)	0.1434 (1)	4.46 (5)
O(5)	0.1841 (3)	0.0931 (2)	0.0253 (1)	4.77 (5)
O(6)	0.3333 (2)	0.3368 (2)	0.0134 (1)	4.48 (5)
C(1)	0.2751 (3)	0.4572 (3)	0.1903 (2)	3.98 (6)
C(2)	0.3536 (3)	0.3645 (3)	0.2344 (2)	3.61 (6)
C(3)	0.3913 (3)	0.2383 (3)	0.2104 (2)	3.43 (6)
C(4)	0.4759 (3)	0.1586 (3)	0.2616 (2)	4.40 (7)
C(5)	0.5128 (4)	0.1988 (4)	0.3306 (2)	4.95 (8)
C(6)	0.4741 (4)	0.3196 (4)	0.3534 (2)	5.46 (8)
C(7)	0.3984 (4)	0.4017 (4)	0.3063 (2)	4.56 (7)
C(8)	−0.0746 (4)	0.3702 (4)	0.0281 (2)	4.75 (7)
C(9)	−0.1178 (3)	0.3463 (4)	0.0959 (2)	4.50 (7)
C(10)	−0.0419 (4)	0.2682 (3)	0.1489 (2)	4.39 (7)
C(11)	−0.0974 (5)	0.2502 (5)	0.2137 (3)	6.5 (1)
C(12)	−0.2189 (5)	0.3117 (6)	0.2242 (3)	8.4 (1)
C(13)	−0.2920 (4)	0.3893 (6)	0.1706 (3)	8.4 (1)
C(14)	−0.2441 (4)	0.4064 (5)	0.1083 (2)	6.3 (1)
C(15)	0.2626 (4)	0.0581 (3)	−0.0178 (2)	4.97 (8)
C(16)	0.3708 (4)	0.1294 (3)	−0.0436 (2)	4.43 (7)
C(17)	0.4021 (4)	0.2631 (3)	−0.0267 (2)	4.13 (7)
C(18)	0.5129 (4)	0.3207 (4)	−0.0563 (2)	4.81 (8)
C(19)	0.5894 (5)	0.2487 (4)	−0.0978 (2)	5.38 (9)
C(20)	0.5601 (4)	0.1177 (4)	−0.1136 (2)	5.74 (9)
C(21)	0.4525 (4)	0.0607 (4)	−0.0886 (2)	5.50 (8)

[a] The displacement of anisotropically refined atoms is given in the form of the equivalent isotropic displacement parameter defined as $^4/_3[a^2\beta_{11} + b^2\beta_{22} + c^2\beta_{33} + ab(\cos\gamma)\beta_{12} + ac(\cos\beta)\beta_{13} + bc(\cos\alpha)\beta_{23}]$.

(26) Cotton, F. A.; Frenz, B. A.; Deganello, G.; Shaver, A. *J. Organomet. Chem.* **1973**, *50*, 227–240.

(27) Crystallographic calculations were carried out by the program package SDP(V3.0), on a PDP-11/60(RSX-11M V4.1), on a VAX-11/780-(VMS V4.4), and on an 8650/8800 VAX cluster (VMS V4.4).

(28) North, A. C. T.; Philips, D. C.; Mathews, F. S. *Acta Crystallogr., Sect. A* **1968**, *24*, 351–359.

thermal parameters are listed in Table VII.

Acknowledgment. Financial supports received from the Department of Science and Technology and the University Grants Commission, New Delhi, India, are gratefully acknowledged. Our special thanks are due to Professor F. A. Cotton for being very helpful.

Registry No. **2** (R = R′ = H), 117227-49-3; 2^+ (R = R′ = H), 117227-54-0; 2^- (R = R′ = H), 117227-59-5; **2** (R = Me, R′ = H), 117227-50-6; 2^+ (R = Me, R′ = H), 117227-55-1; 2^- (R = Me, R′ = H), 117227-60-8; **2** (R = H, R′ = Me), 117227-51-7; 2^+ (R = H, R′ = Me), 117227-56-2; 2^- (R = H, R′ = Me), 117227-61-9; **2** (R = R′ = Me), 117227-52-8; 2^+ (R = R′ = Me), 117227-57-3; 2^- (R = R′ = Me), 117227-62-0; **2** (R = H, R′ = Et), 117227-53-9; 2^+ (R = H, R′ = Et), 117227-58-4; 2^- (R = H, R′ = Et), 117227-63-1; **4** (X = *n*-Bu), 117227-68-6; 4^- (X = *n*-Bu), 117227-74-4; **4** (X = Ph), 117227-79-9; $Ru(bpy)_2CO_3$, 59460-48-9; $[Ru(sal)_2(MeCN)_2]PF_6$, 117227-65-3; $Ru(sal)_2(py)_2$, 117227-71-1; $Ru(sal)_2(PPh_3)_2$, 117227-72-2; $Ru(sal)_2(bpy)$, 117227-73-3; $[Ru(sal)(bpy)_2]ClO_4$, 117227-70-0; $[Ru(sal)_2(bpy)]ClO_4$, 117227-67-5; $Ru(sal)_2(MeCN)_2$, 117227-75-5; $[Ru(sal)_2(py)_2]^+$, 117227-76-6; $[Ru(sal)_2(PPh_3)_2]^+$, 117227-77-7; $[Ru(sal)_2(bpy)]^+$, 117227-66-4; $[Ru(sal)(bpy)_2]^{2+}$, 117227-78-8; salicylaldehyde, 90-02-8; *n*-butylamine, 109-73-9; aniline, 62-53-3; ceric ammonium sulfate, 7637-03-8.

Supplementary Material Available: Complete results of the EPR analysis of RuL_3 (Table VIII) and, for the crystal structure of $Ru(sal)_3$, hydrogen atom positional parameters (Table IX), complete bond distances (Table X) and angles (Table XI), anisotropic displacement parameters (Table XII), torsional angles (Table XIII), least-squares planes (Table XIV), and complete crystallographic data (Table XV) (15 pages); a listing of observed and calculated structure factors (14 pages). Ordering information is given on any current masthead page.

Contribution from the Department of Chemistry and Ames Laboratory, Iowa State University, Ames, Iowa 50011

Concurrent and Reversible Changes of Color and of Phase in an Aqueous Solution of the (2,6-Pyridinedicarboxylato)chloroplatinate(II) Complex. Spectroscopic and Crystallographic Studies of the Discrete Monomer and Evidence of a Stacked Polymer

Xia-Ying Zhou and Nenad M. Kostić*

Received June 30, 1988

The title complex, $[Pt(dipic)Cl]^-$, was prepared in a reaction between dipicolinate salts and $[PtCl_4]^{2-}$. The variation in temperature or in concentration of its aqueous solution causes two changes—of color and of phase—which are sudden, concurrent, and reversible. At higher temperatures or lower concentrations the complex is yellow and monomeric, whereas at lower temperatures or attempted higher concentrations it is red and probably polymeric. The red form is microcrystalline and probably composed of stacked $[Pt(dipic)Cl]^-$ units. Unlike other square-planar complexes that form stacks, the yellow form of $[Pt(dipic)Cl]^-$ remains monomeric over a wide range of concentration and temperature until the sudden onset of the supposed polymerization. The nucleation and growth of the red form are easily monitored owing to the concomitant color change. The monomeric salt $(n\text{-}Bu)_4N[Pt(dipic)Cl]\cdot 0.5H_2O$ crystallizes in the monoclinic (*C*-centered) space group $C2/m$ with the following lattice properties: $a = 19.385$ (6) Å, $b = 27.965$ (9) Å, $c = 19.562$ (3) Å, $\beta = 93.38$ (2)°, $V = 10587$ (8) Å^3, and $Z = 8$. The structure was refined to $R_w = 0.0454$. The $[Pt(dipic)Cl]^-$ ion is essentially planar and contains a Pt(II) atom, a tridentate dipicolinate dianion that forms a strained chelate, and a unidentate Cl^- ligand. The Pt–N distance, on the average 1.89 Å, is uncommonly short. Since the layers of the complex anions are 7.0 Å apart and are separated by the bulky $(n\text{-}Bu)_4N^+$ cations, no intermolecular interactions exist. The putative polymeric form of K[Pt(dipic)Cl] exhibits an X-ray powder pattern different from that of the monomeric $(n\text{-}Bu)_4N^+$ salt. The UV–vis spectrum of the red K[Pt(dipic)Cl] in the solid state contains a low-energy absorption band diagnostic of the stacking. This band disappears when the red polymer dissolves in water to give a yellow monomeric solution. The $[Pt(dipic)Cl]^-$ salts, like thermochromic materials, hold promise as temperature indicators.

Introduction

Discovery and improvement of materials are important aims of chemical research. For example, stacking of planar molecules gives rise to one-dimensional materials, some of which exhibit anisotropic electrical conductivity, cooperative magnetic interactions, metal–insulator transitions, and even superconductivity.[1-4] Study of these properties has brought together chemists, physicists, and materials scientists.

Square-planar complexes of transition metals, particularly those of platinum(II), are notorious for columnar stacking.[1,5-8] When partially oxidized, these stacks become metallic conductors. Most reports on these one-dimensional materials justifiably deal with their properties in the solid state, because it is the solids that are conductive. But the solutions from which these solids are obtained are interesting as well. More should be known about precursors of the one-dimensional polymers,[9] about the mechanism of stacking and polymerization in solution, and about nucleation and growth of the polymers. This knowledge is necessary for a purposeful design and synthesis of new one-dimensional materials.

The first evidence of stacked aggregates, which are precursors for one-dimensional polymers, often is an unusual color dependent on the composition and temperature of the solution. The color variability resembles thermochromism of transition-metal complexes, a phenomenon generally observed in the solid state.[10]

We report here on the unusual behavior of a square-planar platinum(II) complex in solution. It undergoes sudden trans-

(1) Miller, J. S., Ed. *Extended Linear Chain Compounds*; Plenum: New York, 1982; Vol. 1 and 2. *Ibid.* Plenum: New York, 1983; Vol. 3.
(2) Devresse, J. T., Evrard, R., van Doren, V. E., Eds. *Highly Conducting One-Dimensional Solids*; Plenum: New York, 1979.
(3) Miller, J. S., Epstein, A. J., Eds. *Synthesis and Properties of Low-Dimensional Materials*; Ann. N.Y. Acad. Sci. 313; New York Academy of Sciences: New York, 1978.
(4) Interrante, L., Ed. *Extended Interactions Between Metal Ions*; American Chemical Society: Washington, DC, 1974.
(5) Miller, J. S.; Epstein, A. J. *Prog. Inorg. Chem.* **1976**, *20*, 1.
(6) Stucky, G. D.; Schultz, A. J.; Williams, J. M. *Annu. Rev. Mater. Sci.* **1977**, *7*, 301.
(7) Gliemann, G.; Yersin, H. *Struct. Bonding (Berlin)* **1985**, *62*, 87.
(8) Williams, J. M. *Adv. Inorg. Chem. Radiochem.* **1983**, *26*, 235.
(9) Balch, A. L. In *Extended Linear Chain Compounds*; Miller, J. S., Ed.; Plenum: New York, 1982; Vol. 1, Chapter 1.
(10) Bloomquist, D. R.; Willett, R. D. *Coord. Chem. Rev.* **1982**, *47*, 125.

0020-1669/88/1327-4402$01.50/0